GAS HOLDUP AND LONGITUDINAL DISPERSION IN DIFFERENT TYPES OF MULTIPHASE REACTORS AND THEIR POSSIBLE APPLICATION FOR MICROBIAL PROCESSES

J TODT, J LUCKE, K SCHUGERL and A RENKEN

Institut fur Technische Chemie, Technische Universität Hannover, D-3000 Hannover, Callinstr 46, Germany

Abstract—Gas hold-up and liquid phase longitudinal dispersion have been measured in concurrent one- and six-stage two-phase bubble columns as well as in counter-current one-stage two- and three-phase bubble columns To describe the intensity of the longitudinal mixing the logitudinal dispersion and the backflow cell models were applied The possible influence of fluid mixing on microbial processes was investigated

INTRODUCTION

Bubble columns gain increasing importance as gas–liquid reactors for continuous fermentation processes The behaviour of continuous reactor systems has often been represented by the plug flow model, the completely mixed model and the dispersion model These three different models depend on the degree of longitudinal dispersion of media Fermentations are mostly carried out in the conventional stirred-tank type vessel The flow behaviour of many continuous systems lies between the two ideal cases Examples for such models are the axial dispersion model or the N-tanks-in-series model These models contain parameters which describe the degree of longitudinal dispersion

For autocatalytic reactions such as those associated with many biochemical processes Bischoff[1] showed that the choice of the reactor type depends greatly on the desired conversion of substrate to cell At low conversions the stirred-tank reactor is superior to the plug flow reactor, while at high enough conversions a combination of a mixed reactor followed by a plug flow reactor would be the best choice For a given mean residence time of the liquid phase there exists a degree of longitudinal dispersion which gives rise to a maximum conversion Since the performance of a reactor system with autocatalytic kinetics depends on the axial fluid mixing, it is the objective of this work to measure the axial fluid dispersion as a function of the operating conditions for different multiphase systems (Table 1)

APPARATUS

The experimental apparatus (Fig 1) consists of a bubble column with auxiliary equipment for measurements of temperatures, pressures and flow rates, tracer injection

and a recording system for the tracer concentration The column is constructed of six sections For the multistage system a perforated plate with a free area ratio of 0 65% was inserted between each section The bubble column could be operated with either countercurrent or concurrent contact between gas and liquid phases by reversing the liquid flow direction In the counterflow situation the tap water was fed from a storage tank to the top of the column by a centrifugal pump
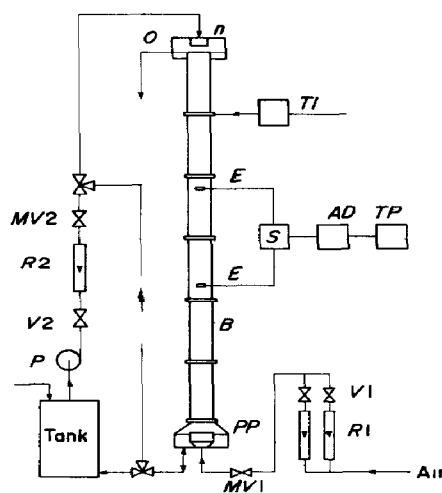
The liquid was uniformly distributed across the cross

Fig 1 Experimental setup B, bubble column, MV, magnetic valve, V, control valve, P, centrifugal pump, R, flow meter, O, flow control, PP, gas distributor (perforated plate), TI, tracer injection, E, electrical conductivity cell, S, scanner, AD, analog digital converter, TP, tape puncher, n, nozzle distributor

Table 1 Investigated multiphase systems

No	Phases	Operation	Stages	Height/cm	Diameter/cm
1	2	concurrent	1	440	14
2	2	concurrent	6	440	14
3	2	countercurrent	1	380	14
4	3	countercurrent	1	380	14

sectional area of the column by means of a nozzle distributor The air passed an oil separator, a pressure control device and entered the column from the bottom through a stainless steel perforated plate distributor The hole diameter of the plate was 0 5 mm, and the free area ratio was 0 25% Flow rates of gas and liquid were measured with calibrated rotameters The superficial gas velocity was varied from $w_{SG} = 0\ 67\text{--}10\ 67$ cm/sec, the superficial liquid velocity from $w_{SL} = 0\ 70\text{--}2\ 38$ cm/sec For the three-phase countercurrent system hollow glass beads (Microballons FT 102, Emerson & Cumming Inc , Mass , U S A) 125–250 μm in diameter were used as solid particles They had a mean density of 0 28 g/cm^3 when measured with water

Liquid axial mixing was measured by pulse tracer technique using a 20% NaCl-solution The tracer was injected into the column through a small stainless steel tube The opening time of the magnetic valve varied between 0 3 and 1 0 secs Concentration of tracer in the reactor was measured at two locations in the column by means of conductivity cells which were installed at a distance of $L = 100$ cm from each other This tracer technique has the advantage that a mathematical perfect pulse is unnecessary The tracer concentration was recorded by data logger on paper tape punch as a discrete function of time The gas hold-up ϵ_G was determined by measuring the pressure drop at several points in the column, and from residence time distributions as well as by measuring the height of the aerated liquid H, and that of the liquid without aeration H_0

$$\epsilon_G = \frac{w_{SG}}{w_G} = \frac{H - H_0}{H} \qquad (1)$$

(For more experimental details see 13)

RESULTS

1 Gas hold-up and relative velocity

In Fig 2 the relative gas fraction is shown as a function of the superficial gas velocity for the investigated systems For all systems gas holdup increases rapidly in the lower range of gas velocities and tends to level off at higher velocities The average gas hold-up in the three-phase system air-tap water-glass beads is higher than in solids-free systems at the same linear liquid velocity, and it increases with the amount of solid particles in the reactor The superficial liquid velocity w_{SL} has only a slight influence on ϵ_G (Fig 3) In countercurrent systems the gas fraction increases with increasing w_{SL}, but decreases in concurrent systems

To compare these results with the ones calculated by some published equations, on Fig 4 the ranges of the ϵ_G-values of the present paper measured in concurrent and counter-current one stage two-phase systems for different liquid flow rates as function of the gas flow rate are plotted together with the ϵ_G-values calculated for the present system by equations of Burkel[14] (curve a), Hugmark[15] (curve b), Mersmann[16] (curve c), Akita[17] (curve d) and Gestrich[18] (curve e)

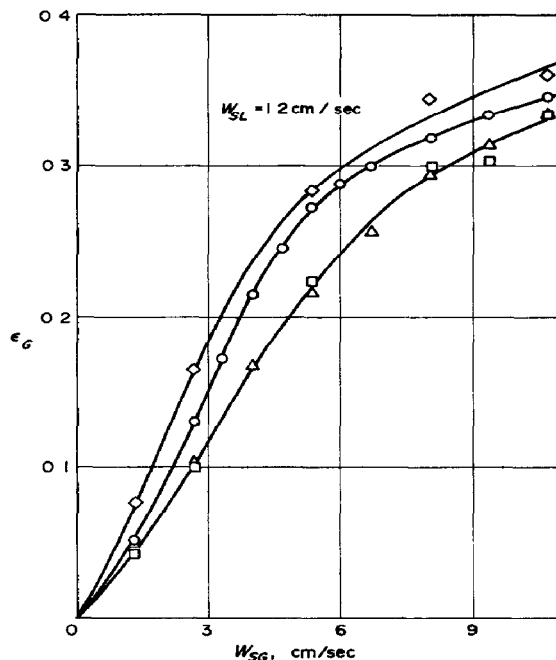One can recognize from Fig 4 that the ϵ_G-values measured on the concurrent one stage-two-phase systems

Fig 2 Gas hold-up as function of the superficial gas velocity $w_{SL} = 1\ 2$ cm/s Two-phase system—counter-current one stage, ○, concurrent one stage, □, multistage, △ Three-phase system—counter-current one stage, ◇
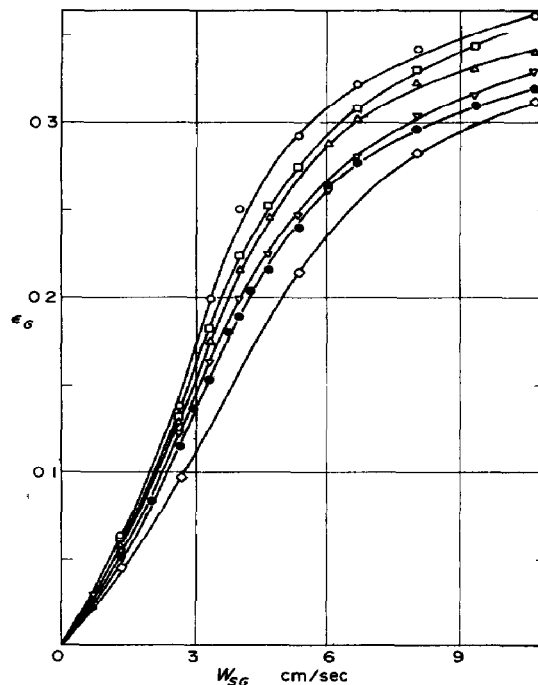

Fig 3 Gas hold-up as function of the superficial gas and liquid velocity One-stage two-phase system concurrent $w_{SL} = 2\ 20$, ◇ Countercurrent $w_{SL} = 2\ 38$ cm/s ○, 1 68, □, 1 20, △, 0 70, ▽, 0, ●

agree with the ones calculated by equation of Gestrich[18] and/or Mersmann[16] only for low and/or high gasflow rates The ϵ_G-values in counter-current systems are between the curves e and c of Gestrich and Mersmann for low gas flow rates and agree partly with the curve c
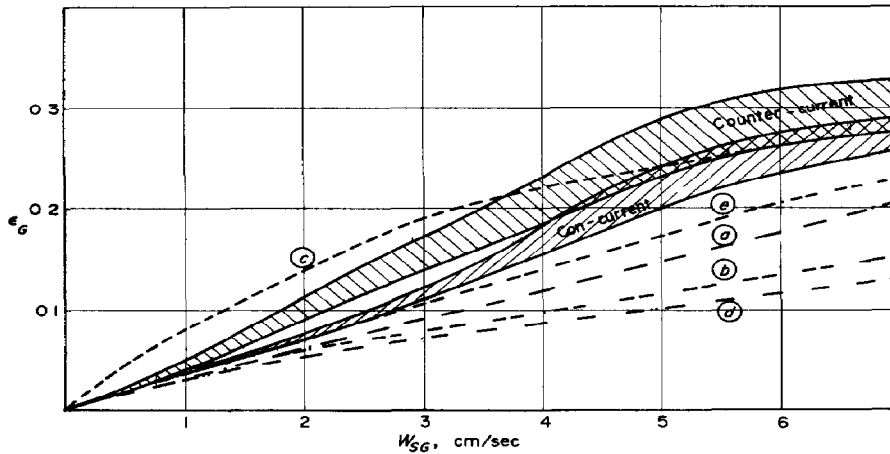
Fig 4 Comparison of the ranges of the ϵ_G-values of the present paper measured in concurrent and countercurrent one-stage two-phase systems for different liquid flow rates as function of the gas flow rate w_{SG} with calculated $\epsilon_0 G$-values according to (a) Burkel[14], (b) Hughmark[15], (c) Mersmann[16], (d) Akita[17], (e) Gestrich[18]
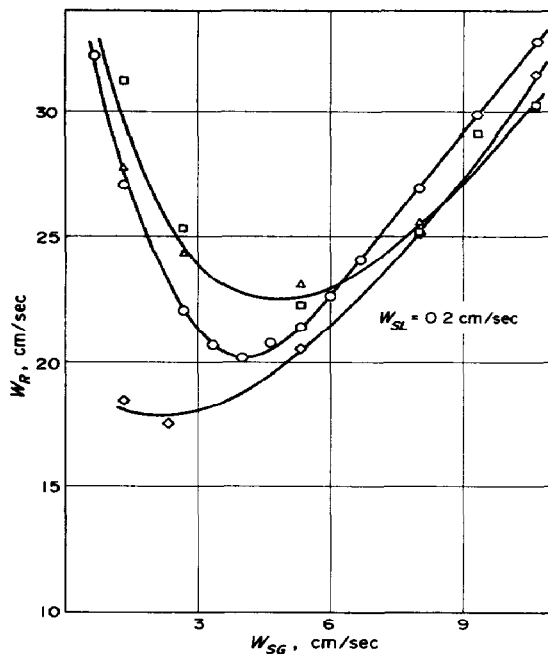

Fig. 5 Relative velocity between gas and liquid as function of the superficial gas velocity $w_{SL} = 1\ 2$ cm/s Two-phase system—countercurrent one stage, O, concurrent one stage, □, multistage, △ Three-phase system—countercurrent one stage, ◇

for high gas flow rates No one of these recommended equations describes the behaviour of ϵ_G in the whole investigated range of gas flow rates, probably because these equations do not consider the influence of different type of gas distributors on the gas holdup ϵ_G

The relative velocity w_R between gas and liquid phase is calculated from hold-up data, the superficial gas and liquid velcoities (+ countercurrent, − concurrent)

$$w_R = w_G \pm w_L = \frac{w_{SG}}{\epsilon_G} \pm \frac{w_{SL}}{1-\epsilon_G} \qquad (2)$$

In Fig 5 the relative velocity measured in the four

systems is plotted against the superficial gas velocity For the two-phase systems the slope of the curves is negative at small values of w_{SG}, and the relative velocity passes through a minimum at a superficial gas velocity of 4–5 cm/sec For superficial gas velocities below 5 cm/sec the bubbles emerging from the perforated plate are characterised by a uniform bubble size distribution and a small average diameter At higher gas velocities the flow is turbulent with random circulation patterns Coalescence increases bubble size which in turn gives a larger effective gas velocity w_G For the three-phase system w_G decreases at small gas rates because of the hindering effect of the solid particles

2 Longitudinal fluid dispersion

Two models were applied to characterise axial mixing effects within the flow reactor the axial dispersion model and the backflow cell model The dispersion model is described by the following dimensionless equation, derived from an unsteady-state material balance on the tracer component[2]

$$\frac{\partial C^*}{\partial \theta} + \frac{\partial C^*}{\partial x^*} = \frac{1}{Pe}\ \frac{\partial^2 C^*}{\partial x^{*2}} \qquad (3)$$

This model is based on the assumption that the two transport mechanisms, bulk flow and longitudinal dispersion, are independent of radial position The dimensionless Peclet-number $Pe = w_L\ L/D_L$ indicates the degree of mixing within within the reactor

The backflow cell model[3] consists of N perfectly mixed cells of equal volume with constant net flow rate V_F and with constant backflow rate V_B from each cell back to the preceding cell The backflow ratio $\beta = V_B/V_F$ and the number of cells N used in this model characterise axial dispersion A material balance for the inert tracer solute in cell i yields an ordinary differential equation

$$\frac{1}{N}\ \frac{dC_i^*}{d\theta} = (1+B)\ C_{i-1}^* - (1+2\beta)\ C_i^* + \beta\ C_{i+1}^* \qquad (4)$$

A set of dimensionless equations is obtained by writing material balances about each cell The parameters Pe or N, β must be determined by experiment A pulse of tracer is injected into the flowing stream, and concentration measurements were taken at two points within the test section, which are far enough from the entrance and exit sections

A widely-used technique for estimating the parameters involves the calculation of the variances of the experimental concentration curves at the two points The difference between them can be related to the parameters

Another way of representing the relation between the two concentration curves is by use of the transfer function concept The model transfer function, which is defined as the ratio between the Laplace-transform of the output divided by the Laplace-transform of the input, can be found by taking the Laplace-transform of each sides of eqns (3) and (4) The system transfer function for the axial dispersion model is[4] (neglecting the end effects)

$$F(s^*, Pe) = \exp\left[\frac{Pe}{2}\left(1 - \sqrt{\left(1 + \frac{4s^*}{Pe}\right)}\right)\right] \quad (5)$$

and for the backflow cell model

$$F(s^*, N, \beta) = \xi N \quad (6)$$

where

$$\xi = \frac{1}{2\beta}\ [(1 + 2\beta + s^*/N)$$
$$- \sqrt{[(1 + 2\beta + s^*/N)^2 - 4\beta\ (1 + \beta)]]}$$

The experimental transfer function can be evaluated from experimental residence time distribution data obtained by numerical integration of the transient response to an imperfect pulse

$$F_M(s^*) = \bar{C}_2^*(s^*)/\bar{C}_1^*(s^*) \quad (7)$$

The model parameters were estimated by a least-squared error analysis of the transformed response data

$$\phi(P_j, s_i^*) = \sum_{i=1}^{n} [F_M(s_i^*) - F(s_i^*, P_j)]^2 \quad (8)$$

The analysis requires that the function $\phi(P_j, s_i^*)$ is minimized with respect to the model parameters $P_j(j = 1, 2, \ldots, m)$ for selected values of the dimensionless Laplace-variable $s^* = s\ \bar{t}$ For the determination of the least-squares estimates the methods of Gauss–Seidel[5] and Marquardt[6] were applied The first method converges rapidly, if the first approximate for the unknown parameters are quite good Otherwise, the method diverges The modified steepest-descent method of Marquardt converges slower than the first method, but has the distinct advantage of converging for almost any first approximate This method seeks to calculate corrections in such a way that at each iteration the value of $\phi(P_j, s_i^*)$ will decrease most rapidly Integer values of s^* ranging from 1 to 5 were used in fitting the data The least-squares method gives directly a numerical estimate of the quality of the fit for different data sets or models

The standard error of estimate is calculated as

$$SE = \sqrt{\left(\frac{\phi(P_j, s_i^*)}{n - m}\right)} \quad (9)$$

where n is the number of data points used for the fit and m the number of parameters The model and the experimental transfer functions are in good agreement The standard deviation of the fitted Peclet-number (Pe = 1 720) is $SE = 2\ 519 \times 10^{-3}$, and of the fitted parameters of the backflow cell model ($N = 24$, $\beta = 13\ 44$) $SE = 2\ 544 \times 10^{-3}$

A relation between the parameters of both models can be obtained by equating the variances of the axial dispersion model and of the backflow cell model[3]

$$Pe = \frac{2N}{1 + 2\beta} \quad (10)$$

Figures 6–8 show the effect of the gas rate on the Peclet-number Pe and the backflow ratio β

For all investigated systems axial dispersion increases with increasing superficial liquid and superficial gas velocities Very high gas rates cause coalescence, and the degree of mixing is considerably increased The intensity of mixing is lower in a multistage bubble column than in the other systems at the same gas rate

Empirical correlations for fluid mixing within the different systems have been derived from the data of this work

$$Pe^*\ w_L \bigg/ \frac{cm}{sec} = B_o\ \left[\frac{w_{SG}}{w_{SL}}\right]^{B_1} \quad (11)$$

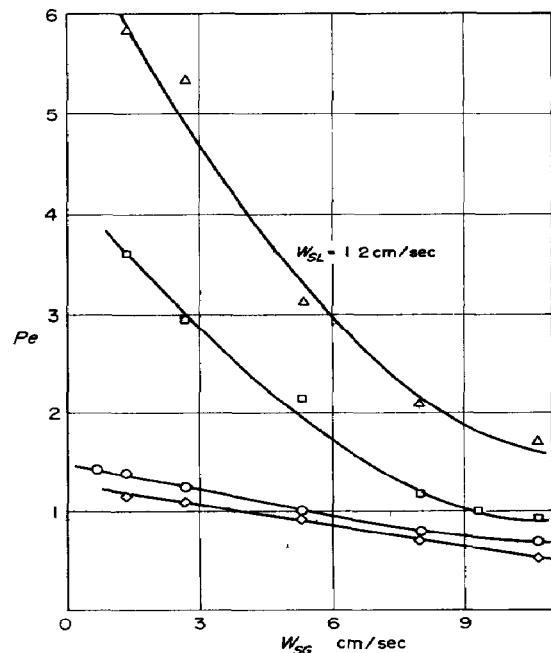The axial dispersion can be characterised by a modified

Fig 6 Effect of the superficial gas velocity on the *Pe*-number Two-phase system $w_{SL} = 1\ 2$ cm/s For symbols see Fig 5
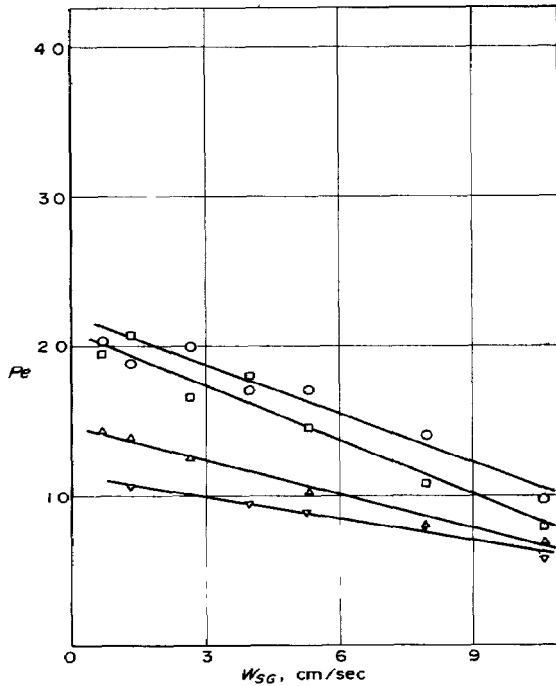
Fig 7 Effect of the superficial gas velocity on the Pe-number for different superficial liquid velocities Two-phase countercurrent, one stage $w_{SL} = 2\,38$ cm/s, $\bigcirc$, 1 68, $\square$, 1 20 cm/s, $\triangle$, 0 71 cm/s, $\triangledown$

Table 2 Parameters of eqn (11)

No	B_0	B_1
1	$14\,577 \pm 0\,423$	$-0\,589 \pm 0\,081$
2	$24\,944 \pm 0\,602$	$-0\,552 \pm 0\,105$
3	$6\,014 \pm 0\,154$	$-0\,307 \pm 0\,034$
4	$2\,551 \pm 0\,061$	$-0\,0044 \pm 0\,0003$
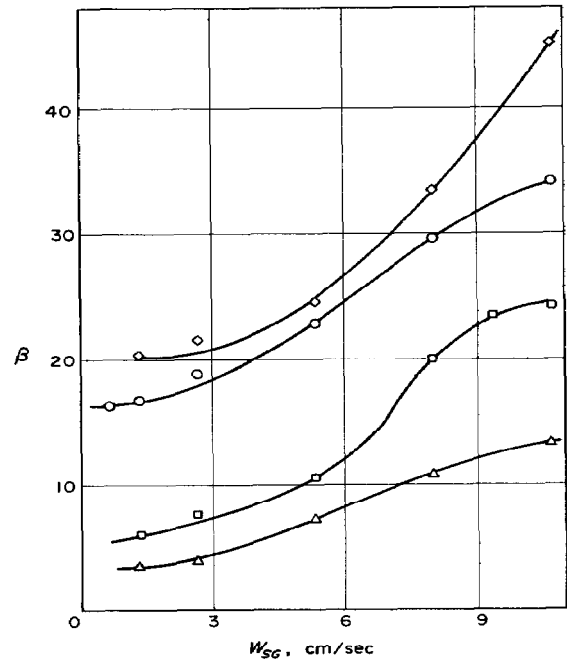
Fig 8 Backflow-ratio β as function of the superficial gas velocity (for symbols see Fig 5)

Peclet-number $Pe^* = w_R \ d/D_L$ based on the column diameter d and the relative velocity w_R This nonlinear equation can be transformed to linear form by taking logarithms of both sides of eqn (11) The parameters B_0 and B_1 of the linear model were estimated by the method of least-squares (Table 2) Fig 9 shows the experimental data and the estimated regression lines The confidence intervals were determined for a significance level of $\alpha = 0\,05[5]$

Figure 10 shows the data $Pe^* \ w_L$ compared with values calculated from eqn (11) Most of the data fall within the dashed lines which represent a mean relative error of

$\pm 20\%$ The results have been compared with the literature data on axial liquid mixing By using the w_{SG}/w_{SL}—values of the published data[7–10] $Pe^* \ w_L$ was calculated by eqn (11) and B_0 and B_1 values of Table 2

By use of the axial dispersion model (3) in conjunction with the Monod growth kinetics[11] the influence of fluid
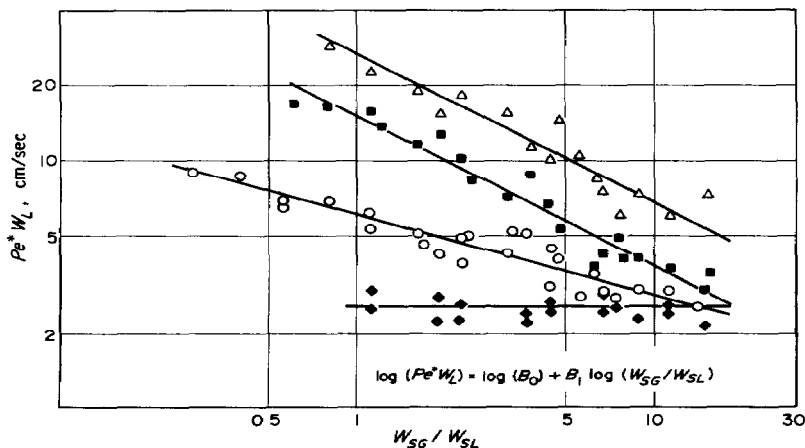

Fig 9 Correlation for the modified Pe-number Two-phase system—countercurrent one stage, $\bigcirc$, concurrent one stage, $\blacksquare$, multistage, $\triangle$ Three-phase system—countercurrent one stage, $\blacklozenge$

mixing on the performance of a microbial process was investigated The performance equations derived from the steady state material balance for substrates and cells were solved by a numerical technique based on the principle of collocation methods [12]

For solving the equations the so-called Danckwerts' boundary conditions were used Figure 11 shows the effect of the Peclet-number on the exit concentration of substrate C^*_{ES} for different Damkohler-numbers $Da = k\ \bar{t}$ The results were obtained by considering following values dimensionless saturation constant $K^* = K/C_{IS} = 0\ 5$, dimensionless initial cell concentration $C^*_{IC} = 0$ At
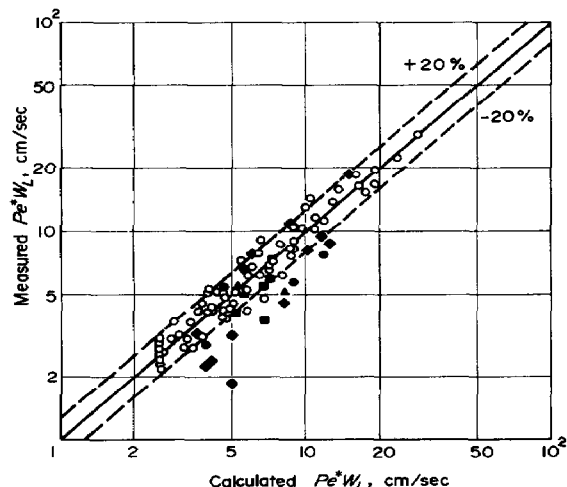
Fig 10 Comparison of experimental and calculated modified
Pe-numbers Langemann[8], ♦, Reith[7], ▲, Argo[9], ■,
Towell[10], ●, present work, ○

low conversions, which correspond lower values of Da, the stirred tank vessel is the most efficient reactor The critical value of Da, for which a stirred tank reactor is still superior to the dispersion model reactor, is 2 37 For any value of Da greater than this critical value the dispersion model reactor is the choice to attain the maximum conversion The optimal Peclet-number is about 1 for $Da = 3$ with a maximum conversion of 76% If the Peclet-number is greater than 6 for $Da = 3$ the growth of cells cannot be maintained The cells tend to be washed out because of insufficient residence time These results show that there exists an optimal Peclet-number (longitudinal fluid dispersion) in a bubble column with autocatalytic kinetics for a given set of Da, C^*_{IC} and K^* ·

As the desired conversion increases a point is reached where a combined system of a stirred tank vessel followed by a plug flow reactor turns out to be an optimum [11] Such a system can be approached by a multi-stage column Recently bubble column fermentors with recycle are recommended because of their favourable fluid-dynamical properties (low energy requirement with regard to their specific surface area) For such systems ($C^*_{IC} > 0$) the optimum Peclet number increases as C^*_{IC} increases if all other parameters remain constant For large values of C^*_{IC} the Peclet number should be as large as possible Since the optimum Peclet number can vary between 0 and ∞ as function of K^*, Da and C^*_{IC}, multi-stage bubble columns with adjusted Pe numbers are in generally superior to one-stage columns

Fig 11 Effect of the *Pe*-number on the exit concentration of substrate for various *Da*-numbers

NOTATION

B_0, B_1	coefficients of eqn (11)
C	tracer concentration, g/cm^3
$\bar{C}(s)$	Laplace-transform of $C(t)$
d	column diameter, cm
D	axial dispersion coefficient, cm^2/sec
Da	Damkohler-number ($Da = k\ \bar{t}$)
F	transfer function
k	maximum specific growth rate when the substrate concentration is not limiting the rate of growth h^{-1}
K	concentration of substrate at which the specific growth rate observed is one half the maximum value
L	distance between the two measuring points, cm
n	number of data points
N	number of cells
P_i	set of parameters
Pe	Peclet-number ($Pe = w_L\ L/D_L$)
Pe^*	modified Peclet-number ($Pe = w_R\ d/D_L$)
s	Laplace-variable, sec^{-1}
t	time, sec
$\bar{t}$	mean residence time, sec
V	volumetric flow rate, m^3/h
w	linear velocity, cm/sec
x	axial distance, cm

Greek symbols

β backflow ratio $(\beta = V_B/V_F)$

ϵ_G gas hold-up

θ dimensionless time

Sub-, Superscripts

1, 2   first, second measuring point

B backward

C cell

E exit

F forward

G gas

I initial

L liquid

S superficial, substrate

$*$ dimensionless variable

REFERENCES

[1] Bischoff K B , *Can J Chem Engng* 1966 **44** 281

[2] Østergaard K and Michelsen M L , *Can J Chem Engng* 1969 **47** 107

[3] Roemer M H and Durbin L D *I & EC Fundl* 1967 **6**(1) 120

[4] Michelsen M L and Østergaard K , *Chem Engng Sci* 1970 **25** 583

[5] Himmelblau D M , *Process Analysis by Statistical Methods* J Wiley, New York 1970

[6] Marquardt D W , *Chem Engng Prog* 1959 **55**(6) 65

[7] Reith T Renken S and Israel B A , *Chem Engng Sci* 1958 **25** 619

[8] Langemann H and Taubert C , *Verfahrenstechn* 1968 **2** 417

[9] Argo W B and Cova D R *I & EC Proc Des Develop* 1965 **4** 352

[10] Towell G D and Ackermann G H , *Fifth European, Sec Intern Symp on Chem React Engng* (1972)

[11] Chen G K C , Fan L T and Erickson L E , *Can J Chem Engng* 1972 **50** 157

[12] Fan L T , Chen G K C and Erickson L E , *Chem Engng Sci* 1971 **26** 379

[13] Todt J , Dissertation, TU Hannover 1974

[14] Burkel W , *Chem Ing Techn* 1974 **46** 205

[15] Hughmark G A , *Ind Engng Chem Process Des Dev* 1967 **6** 218

[16] Mersmann VDI-Forschungsheft 491 VDI-Verlag Düsseldorf 1962

[17] Akita K and Yoshida F , *Ind Engng Chem Proc Des Dev* 1973 **12** 76

[18] Gestrich W and Rähse W , *Chem Ing Techn* 1975 **47** 8